

Classical Trajectory Perspective on Double Ionization Dynamics of Diatomic Molecules Irradiated by Ultrashort Intense Laser Pulses

Di-Fa Ye^{1,2}, Jing Chen¹, and Jie Liu^{1,*}

1. Institute of Applied Physics and Computational Mathematics, Beijing 100088, P. R. China

2. Graduate School, China Academy of Engineering Physics, Beijing 100088, P. R. China

In the present paper, we develop a semiclassical quasi-static model accounting for molecular double ionization in an intense laser pulse. With this model, we achieve insight into the dynamics of two highly-correlated valence electrons under the combined influence of a two-center Coulomb potential and an intense laser field, and reveal the significant influence of molecular alignment on the ratio of double over single ion yield. Analysis on the classical trajectories unveils sub-cycle dynamics of the molecular double ionization. Many interesting features, such as the accumulation of emitted electrons in the first and third quadrants of parallel momentum plane, the regular pattern of correlated momentum with respect to the time delay between closest collision and ionization moment, are revealed and successfully explained by back analyzing the classical trajectories. Quantitative agreement with experimental data over a wide range of laser intensities from tunneling to over-the-barrier regime is presented.

PACS numbers: 33.80.Rv, 34.80.Gs, 42.50.Hz

I. INTRODUCTION

Atoms and molecules exposed to high-intensity ultrashort laser pulses have been attracting much attention during the past ten years and plenty of striking phenomena emerged such as multiphoton ionization (MPI), above threshold ionization (ATI), high order harmonic generation (HHG) and nonsequential double ionization (NSDI) [1, 2]. The dynamics behind the NSDI is most complicated because it deals with two highly entangled valence electrons [3]. In contrary to the situation of single ionization where the experimental data can be accurately predicted by the single active electron (SAE) model [4], the NSDI data are usually higher by many orders of magnitude than the sequential Ammosov-Delone-Krainov (ADK) tunneling theory that bases on the SAE approximation. This fact suggests that the electron-electron correlation plays a crucial role in NSDI physics. Diverse correlation mechanisms like the shake-off [5] and the recollision [6, 7] were proposed to account for the electron correlation in the experimental observations. It is commonly believed now that the rescattering is the dominant mechanism for the excessive atomic double ionization (DI) yields [8].

Compared to atomic case, the NSDI in the molecules is more complicated because of the additional freedom that molecules have [9, 10]. In addition to the typical strong-field phenomena like excessive DI yields in the tunneling regime, high harmonic generation of the driving laser field, and momentum correlation between the two emitted electrons, some new phenomena such as bond softening [11], zero photon dissociation [12], and alignment dependence of DI yield [13, 14, 15] were observed in recent molecular experiments.

However, these experimental data for molecular double ionization is far from well understood in theory. The complex dynamics of correlated $e - e$ pair responding to two-center nuclear attraction and laser force poses a great challenge to any quantum theoretical treatment. For instance, a fully-dimensional quantum-mechanical computation from first principle is very very time expensive even for the simpler case of highly symmetric atoms [16]. This leaves approximate approaches developed recently, such as one-dimensional quantum model [17], many-body S-matrix [18] and simplified classical methods [19]. In either case, the complex electron dynamics which is crucial for molecular DI is not fully explored and the theoretical results can not account for experimental data quantitatively.

In this paper, we explore a feasible semiclassical theory, following the treatment in our recent Letter [20], extending the calculations and presenting a more detailed account of the theoretical methodology.

Our calculation is capable of quantitatively reproducing the unusual excess DI yield of nitrogen molecules for a wide range of laser intensities from $5 \times 10^{13} \text{W/cm}^2$ to $1 \times 10^{15} \text{W/cm}^2$. The significant influence of molecular alignment on DI yield is virtually revealed: i) The ratio between double and single ionization yield is less for perpendicular molecules than that of parallel molecules; ii) This anisotropy becomes more dramatic if the molecules are irradiated by a shorter laser pulse. In particular, our model provides an intuitive way of understanding the complex dynamics involved in the molecular DI with back analyzing the classical trajectories. Their sub-cycle energy evolution verify that collisions between electrons determines the fate of molecular DI, therefore consolidate the classical rescattering view of molecular DI. Statics based on plenty of individual trajectories show that electrons are most likely to be emitted at 30° off laser peak, indicating the accumulation of emitted electron pairs at $k_1^{\parallel} = k_2^{\parallel} = \pm 0.5 a.u.$ in the first and third quadrants

*Email: liu'jie@iapcm.ac.cn

of parallel momentum plane $(k_1^{\parallel}, k_2^{\parallel})$, which is consistent with the experimental results. Moreover, the ejected electrons emerge in the same momentum hemisphere and opposite momentum hemisphere alternately, depending on whether the delayed time between closest collision and ionization is odd or even half laser cycles.

Our paper is organized as follows. In Sec.II we present our semiclassical quasi-static model. Calculations on double ionization yield for nitrogen molecules are presented and compared with experimental data in Sec.III. In Sec.IV, we give an analysis on the classical trajectories and unveil sub-cycle dynamics of the molecular double ionization. Sec.V is our conclusions and discussions.

II. MODEL

We consider a diatomic molecule with two valence electrons irradiated by a laser field whose temporal and spatial distribution (see Fig.1(a)) is expressed as

$$\varepsilon(t) = \varepsilon_0(R_L, Z_L) \sin^2\left(\frac{\pi t}{nT}\right) \cos(\omega t) \mathbf{e}_z. \quad (1)$$

In experiments, molecules are driven through the laser beam perpendicularly. Thus the external field along the propagation direction of the laser beam is approximately constant and in the lateral direction it can be treated as an ideal Gaussian beam, i.e., $\varepsilon_0(R_L, Z_L) = \varepsilon_0(R_L) = \varepsilon_0 \exp(-R_L^2/R_0^2)$, where ε_0 is the peak laser field, R_L represents the position of the molecules in the laser beam, and R_0 is the radius of the beam. The maximum of R_L is chosen to be three times or more of R_0 to ensure the convergence of our results. A \sin^2 enveloped laser with the full width of nT is used in our calculations, where T and ω are period and angular frequency of the laser field respectively and n denotes the number of optical cycles.

In quantum mechanics, ionization processes are described by the evolution of wave packets, however, in our model they are traced by launching a set of trajectories with different initial parameters instead (To some extent, the distribution of these parameters can be regarded as an alternative emulation of quantum mechanics). For a certain trajectory, the evolution of two electrons can be described by classical Newton equations:

$$\frac{d^2 \mathbf{r}_i}{dt^2} = \varepsilon(t) - \nabla(V_{ne}^i + V_{ee}). \quad (2)$$

Here $\varepsilon(t)$ is the external laser field discussed above. The index i denotes the two different electrons. V_{ne}^i and V_{ee} are Coulomb interaction between nuclei and electrons and between two electrons, respectively.

$$\begin{aligned} V_{ne}^i &= -\frac{1}{r_{ai}} - \frac{1}{r_{bi}}, \\ V_{ee} &= \frac{1}{|\mathbf{r}_1 - \mathbf{r}_2|}, \end{aligned} \quad (3)$$

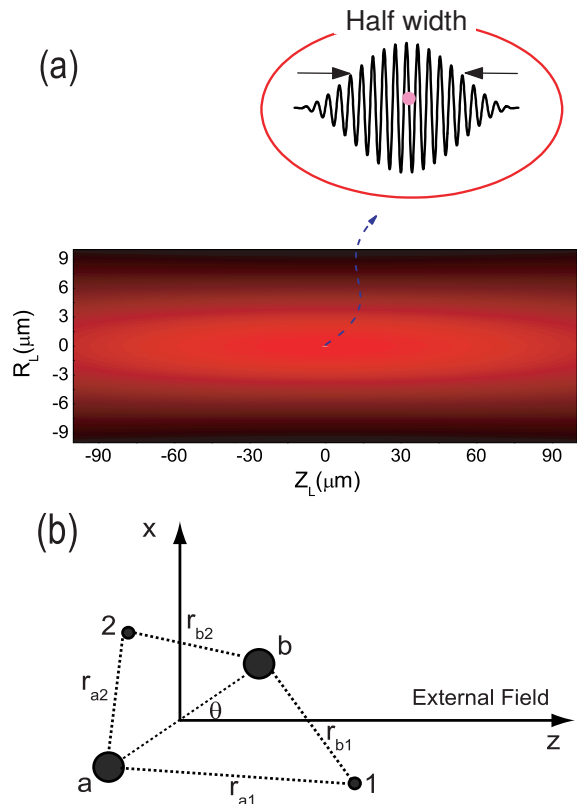


FIG. 1: (color online). (a) The spacial and temporal profile of a typical laser beam, (b) The coordinate system adopted in our paper.

where r_{ai} and r_{bi} are distances between the i th electron and nucleus a and b , respectively (as shown in Fig.1(b)).

To solve the Newton equations, we need the initial conditions of the two electrons, including the initial time, initial position and momentum. Their distribution are quite different for the tunneling and over-the-barrier regime due to the different ionized mechanism of the first electron.

A. Tunneling regime

In the long-wavelength limit, the laser field varies slowly in time and can be regarded as a quasi-static field compared with valence electron's circular motion around nuclei. Under this field, the Coulomb potential between nuclei and electrons is significantly distorted. When the instantaneous field (at time t_0) is sufficient strong but still smaller than a threshold value (see Fig.2(a)), one electron is released at the outer edge of the suppressed Coulomb potential through quantum tunneling with a rate $\varpi(t_0)$ given by molecular ADK formula[21].

The electron tunnels out through a saddle point[19] directing to a channel of the local minimum in the com-

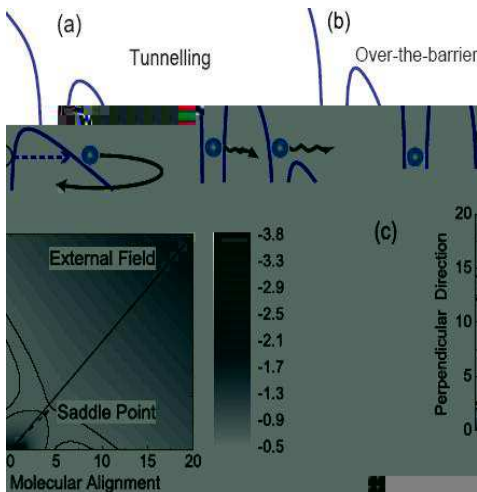


FIG. 2: (color online). (a) Tunneling ionization. (b) Over-the-barrier ionization. (c) The contour plot of the combined Coulomb potential and external laser field. It clearly shows that the saddle point locates approximately along the direction of the external field.

bined potential of the Coulomb interaction and the external field (see, Fig.2(c)). Because the difference between the direction of the saddle point and the external field is very small, we safely regard the external field direction (z axis) as the tunnelling direction. Thus, the initial position of the tunnelled electron can be derived from following equation,

$$-\frac{1}{r_{a1}} - \frac{1}{r_{b1}} + \int \frac{|\Psi(\mathbf{r}')|^2}{|\mathbf{r}_1 - \mathbf{r}'|^2} d\mathbf{r}' + I_{p1} - z_1 \varepsilon(t_0) = 0, \quad (4)$$

with $x_1 = y_1 = 0$. The wavefunction Ψ is given by the linear combination of the atomic orbital-molecular orbital (LCAO-MO) approximation. Taking N_2^+ for example, we choose $\phi(r) = \frac{\lambda^{3/2}}{\sqrt{\pi}} e^{-\lambda r}$ as the trial function to construct the molecular orbital $\Psi(r) = c[\phi(r_{a2}) + \phi(r_{b2})]$, where c is the normalization factor. The parameter λ , which equals to 1.54 for N_2^+ , is determined through variational approach. That is, calculate the variational energy for the given wavefunction and assume it equals to the second ionization energy of the molecule. The initial velocity of tunnelled electron is set to be $(v_\perp \cos \varphi, v_\perp \sin \varphi, 0)$, with v_\perp having the same distribution as that in atomic case, i.e.,

$$w(v_\perp) dv_\perp = \frac{2(2I_{p1})^{1/2} v_\perp}{\varepsilon(t_0)} \exp\left(-\frac{v_\perp^2 (2I_{p1})^{1/2}}{\varepsilon(t_0)}\right) dv_\perp, \quad (5)$$

where φ is the polar angle of the transverse velocity uniformly distributed in the interval $[0, 2\pi]$.

In order to get the initial velocity distribution, we employ a technique widely used in classical Monte Carlo (MC) simulation. Firstly, we generate two random number v_\perp^{test} and w_{test} in the interval $[0, v_\perp^{\max}]$ and

$[0, w_{\max}]$, respectively. If $w(v_\perp^{test}) > w_{test}$, v_\perp^{test} is kept as the initial transverse velocity, otherwise it is rejected and the above procedure is repeated.

For the bound electron, the initial position and momentum are depicted by single-electron microcanonical distribution (SMD) [23],

$$F(\mathbf{r}_2, \mathbf{p}_2) = k\delta[I_{p2} - \mathbf{p}_2^2/2 - W(r_{a2}, r_{b2})], \quad (6)$$

where k is the normalization factor, I_{p2} denotes the ionization energy of molecular ions such as N_2^+ , and $W(r_{a2}, r_{b2}) = -1/r_{a2} - 1/r_{b2}$ is the total interaction potential between the bound electron and two nuclei.

B. Over-the-barrier regime

The above scheme is in the spirit of our quasi-static model for atomic DI [24] and is applicable only when the instantaneous laser field is weaker than the threshold value [25]. To give a complete description of the DI of molecular system for the whole range of laser intensities (see Fig.4), one needs to further extend the above model to over-the-barrier regime (Fig.2b, in such case Eq.(4) has no real roots). This is done by constructing the initial conditions with double-electron microcanonical distribution (DMD) [26], i.e.,

$$F(\mathbf{r}_1, \mathbf{r}_2, \mathbf{p}_1, \mathbf{p}_2) = \frac{1}{2}[f_\alpha(\mathbf{r}_1, \mathbf{p}_1)f_\beta(\mathbf{r}_2, \mathbf{p}_2) + f_\beta(\mathbf{r}_1, \mathbf{p}_1)f_\alpha(\mathbf{r}_2, \mathbf{p}_2)], \quad (7)$$

with

$$f_{\alpha,\beta}(\mathbf{r}, \mathbf{p}) = k\delta[I_{p1} - \frac{\mathbf{p}^2}{2} - W(r_a, r_b) - V_{\alpha,\beta}(\mathbf{r})], \quad (8)$$

where $V_{\alpha,\beta}(\mathbf{r})$ represents the mean interaction between two electrons, $V_{\alpha,\beta}(\mathbf{r}) = \frac{1}{r_{b,a}}[1 - (1 + \kappa r_{b,a})e^{-2\kappa r_{b,a}}]$. κ can be obtained by a variational calculation of the ionization energy of molecules ($\kappa = 1.14$ for N_2). Details can be found in Ref.[26].

We would like to give some remarks here. (i) In our calculations, the trajectories obtained from DMD are weighed by $\varpi(t_0)$ [21]. (ii) Part of the electrons obtained from DMD could "self-ionize" even without the presence of external field. To avoid such a unphysical self-ionization, we evolve the electrons for several optical cycles freely and abandon those samples whose energy are greater than zero during the free evolution process. (iii) The initial total energy distribution of the two electrons is plotted in Fig.3, where we see a long tail on both sides. They are cut off by introducing two parameters E_{min} and E_{max} , which satisfy

$$\frac{\int_{E_{min}}^{E_{max}} E \rho(E) dE}{\int_{E_{min}}^{E_{max}} \rho(E) dE} = E_M, \quad (9)$$

where $E_M \approx I_{p1} + I_{p2}$ is the most probable energy and $\rho(E)$ is the state density around E .

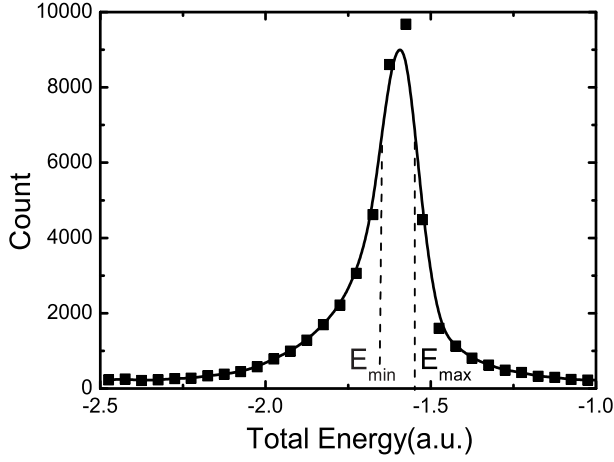


FIG. 3: Total energy distribution of the two electrons. E_{min} and E_{max} are used to cut off the long tail. Only the electrons with a total energy between E_{min} and E_{max} is adopted in our calculation.

With the above initial conditions, the Newtonian equations are solved using the 4-5th step-adaptive Runge-Kutta algorithm and DI events are identified by energy criterion. In our calculations, more than 10^5 weighted (i.e. by rate $\varpi(t_0)$) classical trajectories of electron pair are traced and a few thousands or more of DI events are collected for statistics. Convergency of the numerical results is further tested by increasing the number of launched trajectories twice.

III. CALCULATION ON THE DI OF N_2 : COMPARISON WITH EXPERIMENTS

In this section, we apply our theory to the nitrogen molecules and compare our model calculation with experimental data. The parameters are chosen to match the experiments, *e.g.* the internuclear separation is $2.079a.u.$, the first and second ionization energy are $I_{p1} = 0.5728a.u.$, $I_{p2} = 0.9989a.u.$, respectively. The laser frequency is $\omega = 0.05695a.u.$ corresponding to a wavelength of $800nm$. Based on our model, we successfully reproduce the plateau representing the excessive DI yields due to the correlation between electrons, and reveal a slight shallow dip at intensity of $0.4 \times 10^{15}W/cm^2$ indicating a transition point below which the electron correlation plays role. In addition, our model calculations confirm the dramatic dependence of DI yield on molecular alignment. In Fig.4, the ratio between double and single ionization yield is plotted with respect to the peak laser intensities from $5 \times 10^{13}W/cm^2$ to $1 \times 10^{15}W/cm^2$. The number of optical cycle is chosen as 37 to match the experiments of Cornaggia [10]. Our numerical results show good agreement with the experimental data over the whole range, thus confirm the validity of our model. The curve can be clearly divided

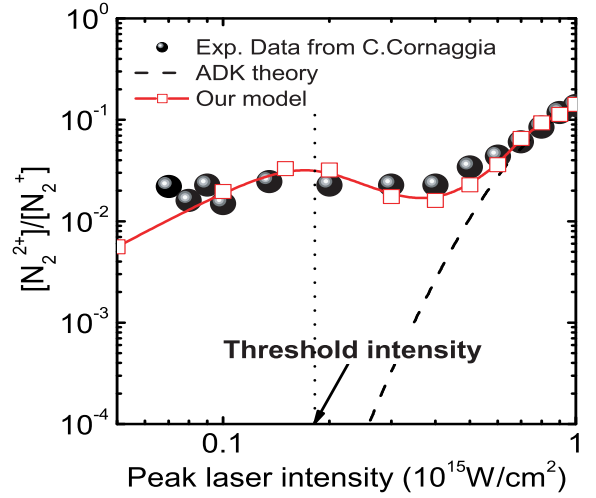


FIG. 4: Comparison between DI data[10] and theory for nitrogen molecule. $0.185 PW/cm^2$ is the threshold intensity separates the tunneling regime and over-the-barrier regime as schematically plotted in Fig.2. To our knowledge, the results from our theoretical model are the first to be in good agreement with experimental data for a wide range of laser intensities from tunneling regime to over-the-barrier regime.

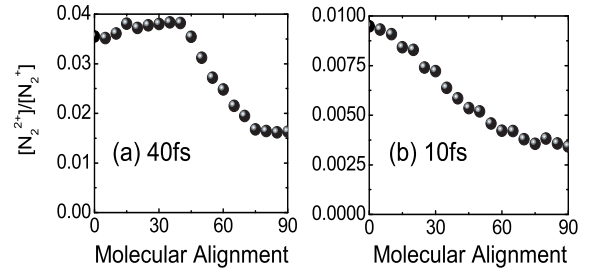


FIG. 5: The molecular alignment dependence of DI ratios for laser intensity of $0.15PW/cm^2$.

into three parts: the low intensity regime ($5 \times 10^{13}W/cm^2$ to $1.85 \times 10^{14}W/cm^2$), where tunneling ionization plays an important role; the very high intensity regime ($5 \times 10^{14}W/cm^2$ to $1 \times 10^{15}W/cm^2$) which can be also well described by ADK theory, indicating that the electrons are pulled out sequentially. In particular, there exists a plateau (moderate intensity) regime with a shallow dip, which can be seen from the corresponding experiments in Ref.[10] Fig.10. Back analysis about classical trajectories indicates that the underlying dominant mechanism in these three regimes are widely divergent as will be shown latter.

In our producing data in Fig.4 the molecular alignment is set to be random and our result is obtained by averaging over different orientations. However, the inherent nuclear degrees of freedom of molecules do manifest themselves as the significant alignment effect in our model. On the other hand, recent progress in experimental tech-

nique has make it possible to control molecular alignment by applying a weak pre-pulse [15]. With these considerations and further application of our model, we calculate the ratios between double and single ionization according to different angles between molecular alignment and laser polarization. Main results are presented in Fig.5. It clearly shows two tendencies, i) The ratio between double and single ionization yield is less for perpendicular molecules than that of parallel molecules; ii) This anisotropy becomes more dramatic when the molecules are irradiated by a shorter laser pulse.

Compared with shorter pulse case, Fig.5(a) shows the ratios between double and single ionization keeps almost a constant until 35° and then decreases rapidly. At 90° (i.e., perpendicular case), the ratio become half of that in parallel case. This result is qualitatively in agreement with experimental data [15]. Quantitatively, our factor 2 is larger than the observed ratio of 1.1 between parallel and perpendicular case [15]. This discrepancy comes from the unperfect control of molecular alignment in practical experiments due to the rotation of molecules and many other uncertain factors. Based on our theoretical results, a simple estimation will conclude that only about 15% of the molecules are "switched" to the appointed direction additionally. Further explorations show that molecular alignment also significantly affects the correlated momentum distribution of emitted electrons. Details will be presented elsewhere [22].

IV. SUB-CYCLE DYNAMICS OF MOLECULAR DI

With our model we are capable to extract vital information by tracing back the history of individual DI trajectories[27]. Such classical trajectory perspective provides us an intuitive way towards understanding the complex dynamics involved in molecular DI.

A. Typical trajectories responsible for emitting electron pairs

In Fig.4, the vertical dot line indicates the threshold value of 0.185 PW/cm^2 , which separates the double ionization data into two parts, the tunneling regime and over-the-barrier regime. When peak laser intensity is below this value, there exist two dominant processes responsible for emitting both electrons, namely, collision-ionization(CI) and collision-excitation-ionization(CEI), as shown in Fig.6(a)(b), respectively. The unique feature of these two mechanism is that the first electron tunnels out through the potential barrier and escapes instead of being pulled out directly by the laser field. This tunneling mechanism can't be included by any classical theory, thus we have not choice but place an electron outside the barrier directly. As a result, we usually notice that the tunneled electron has a higher initial energy as shown in

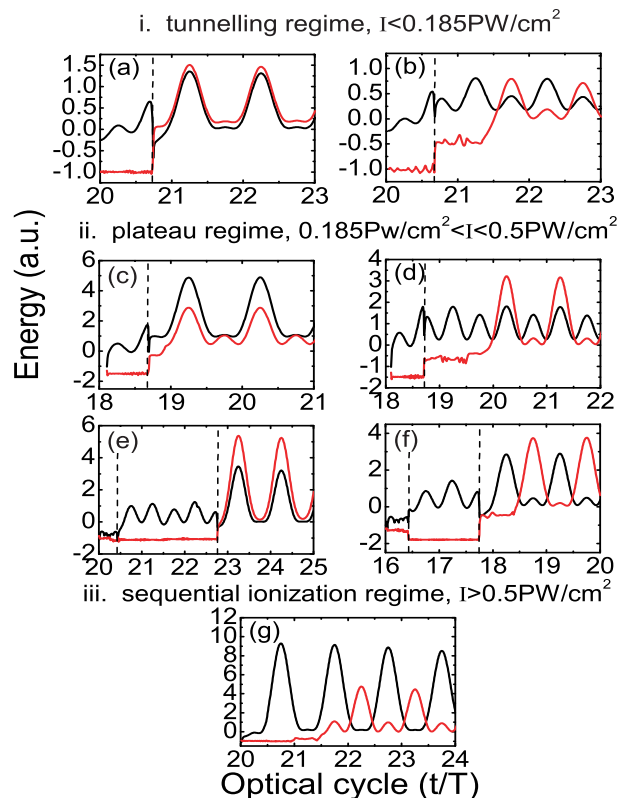


FIG. 6: (color online). Typical energy evolution of the electron pair in three different regimes: (i) tunneling regime, (ii) plateau regime and (iii) sequential ionization regime. Vertical dashed lines indicate the moment when significant collision between two electrons emerge.

Fig.6(a) and (b); while in other trajectories, the two electrons almost have the same initial energy, a reflection of the identity. For CI, the tunneled electron is driven back by the oscillating laser field to collide with the bounded electron near its parent ions causing an instant (\sim attosecond) ionization. The condition for occurrence of CI is usually hard to reach. It requires the kinetic energy of the returned electron exceeds the ionization energy of the bound electron and they should move close to each other to share the excess kinetic energy. However, as pointed out by other numerical studies, the returning trajectories can be assumed to be a freely spreading Gaussian wave packet whose return width is about 30 a.u. [28]. So most of the cases, the returned electron just slides apart from the bound electron and only contribute a little proportion of its kinetic energy to the inner one, in this case CEI occurs instead. For CEI, the inner electron is firstly excited through collision with the returned electron, then undergoes a time-delayed (\sim a few optical periods) field ionization of the excited state. During the time interval, the returned and escaped again electron oscillates in the laser field like a near-free electron while the excited but still bounded electron move around the cores until accumulate enough energy to cause DI.

When the instantaneous laser field is above the threshold value, over-barrier ionization emerges. In this regime we observe more complicated trajectories for DI processes. Except for CI (Fig.6(c)) and CEI (Fig.6(d)) trajectories similar to tunneling cases, there are multiple-collision trajectories as shown in Fig.6(e),(f) as well as collisionless trajectory of Fig.6(g). In Fig.6(e) and (f), two valence electrons entangle each other initially, experience a multiple-collision and then emitted. These two kinds of trajectories exits around the threshold intensity where the over-barrier ionization start to emerge but the external field is not strong enough to pull out the electron immediately without the assistant of Coulomb repulsion between two electrons. The four types of trajectories indicated by Fig.6(c-f) represent the dominant processes of DI in the plateau regime from $0.185\text{PW}/\text{cm}^2$ to $0.5\text{PW}/\text{cm}^2$, which are much more complicated than that of tunneling regime, but still accompanied by once or multiple times of collisions between two electrons [29]. However, above $0.5\text{PW}/\text{cm}^2$, the double ionization is dominated by a collisionless sequential ionization whose typical trajectory is represented by Fig.6(g). In this regime, our numerical results tend to ADK theory.

B. Time delay effect on correlated momentum

A key feature distinguishing classical (or semi-classical) model from quantum-mechanical treatment is the most conspicuous and least ambiguous implication of three time scale during the history of individual DI trajectories [30], i.e., the time of single ionization, the time of closest collision and the time of DI. The time of single ionization is adopted as the start time of our simulation, and determines the weight of each trajectory. After single ionization, the electron travel much of the time in the intense laser field like a classical object until recollide with the bound electron, thus lead to DI eventually. Usually, there is a time lag between the time of DI and closest collision. Such time delay determines the fate of two electrons, and is also firmly related to the final parallel momentum.

Like the atomic cases, a simplified model[24] neglecting most of the unimportant factors, such as the spacial distribution of the laser beam and temporal envelop of the laser pulse, would be more convenient while still give clear interpretation to most of the phenomena. So in this section, we assume the molecules are exposed to a cosine external field and the first electrons tunnelled out in the first half optical cycle. The electric field is switched off using a \cos^2 envelope during two optical cycles at last. As we would discuss later, many important information can be extracted from the distribution of laser phase at the moment of closest collision and ionization [31, 32]. We choose three typical laser intensities, i.e. $0.12\text{PW}/\text{cm}^2$, $0.4\text{PW}/\text{cm}^2$ and $1\text{PW}/\text{cm}^2$, representing the tunneling regime, plateau regime and sequential ionization regime, to analyze in detail.

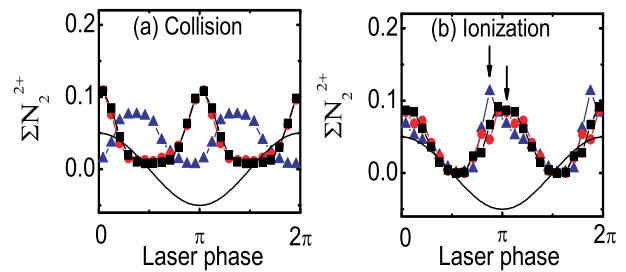


FIG. 7: (color online). DI yield vs laser phase when (a) the two electrons become closest; (b) both the electrons are ionized, at different laser intensity $0.12\text{PW}/\text{cm}^2$ (triangle), $0.4\text{PW}/\text{cm}^2$ (circle) and $1\text{PW}/\text{cm}^2$ (square), respectively. The solid lines represent the laser field.

Fig.7(a) shows the diagram of DI yield versus laser phase at the moment of closest collision. In the tunneling regime (i.e., $0.12\text{PW}/\text{cm}^2$), we note that the collision can occur throughout most of the laser cycle and the peak emerges slightly before the zeroes of the laser field, consistent with the prediction of simple-man model[6] and recent results from purely classical calculation[27]. However, for other two cases, the collision between two correlated electron turns to occur mainly at peak laser field. This is because ionization mechanism changes at the transition to over-the-barrier regime, where both electrons rotate around nuclei initially and they usually become closest before one of them is driven away by the external field (laser peak) rather than during the recollision process (zeroes of the laser field).

Fig.7(b) confirms that most DI occurs around the maximum of laser field for both tunneling regime and over-the-barrier regime. More interestingly, compared to two other cases we observe a peak shift of $\sim 30^\circ$ off the field maximum for the tunneling case. It is due to the larger fraction of CI trajectories in this regime. With assuming that the colliding electrons leave the atom with no significant energy and electron-electron momentum exchange in final state is negligible (these assumptions have been checked by directly tracing trajectories), the parallel momentum $k_{1,2}^{\parallel}$ of each electron results exclusively from the acceleration in the optical field: $k_{1,2}^{\parallel} = \pm 2\sqrt{U_p} \sin \omega t_{ion}$ [32]. The above shifted peak indicates the accumulation of the emitted electrons at $k_1^{\parallel} = k_2^{\parallel} = \pm 0.5 a.u.$ in the first and third quadrants of parallel momentum plane $(k_1^{\parallel}, k_2^{\parallel})$. It is consistent with the experimental data of Ref.[15] (see their Fig.2).

Usually, there is a time delay between closest collision and ionization. Fig.8 shows the profound effects of time delay on correlated momentum, where the phase angle of momentum vector $(k_1^{\parallel}, k_2^{\parallel})$ is introduced to describe the correlation between two electrons' momentum: $[0, \pi/2]$ and $[\pi, 3\pi/2]$ correspond to a same-hemisphere emission while $[\pi/2, \pi]$ and $[3\pi/2, 2\pi]$ correspond to a opposite-hemisphere emission. In all three cases we observe a

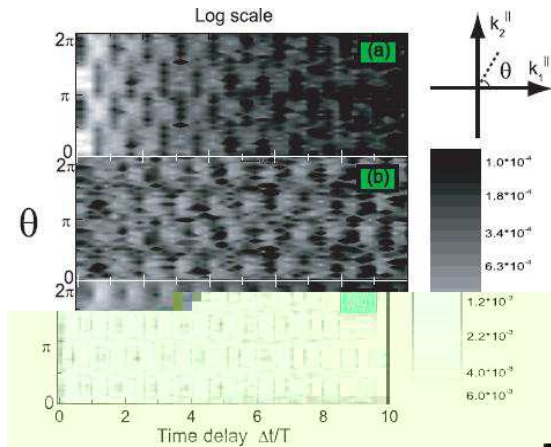


FIG. 8: (color online). The relationship between the correlated momentum and the delay time at (a)0.12PW/cm² (b)0.4PW/cm² (c)1.0PW/cm²

long-tail up to several optical cycles. For the sequential ionization of 1 PW/cm², it means after one electron is deprived from nuclei by laser fields the other electron is slowly (i.e. waiting for up to a few optical cycles) ionized. In the tunneling regime, the long-tail indicates that CEI mechanism is very pronounced for the molecular DI (contribute to 80% of total DI yield). This observation is different from purely classical simulation [27], where CI effect is believed to be overestimated. Our results, however, are consistent with experiments of Ar atom [31], where the ionization energy and laser field parameters are close to our case. The reason is stated as follows. For the intensity of 0.12PW/cm², the maximal kinetic energy of the returned electron is $3.17U_p = 0.85a.u.$, still smaller than the ionization energy of N_2^+ . Even with the assistance of the Coulomb focusing [6, 7], it is still not easy for the returned electrons to induce too many CI events.

Furthermore, such time delay might provide more physics beyond simple rescattering scenario. Recently a statistical thermalization model has been proposed for the nonsequential multiple ionization of atoms in the tunneling regime [33]. This model shows that sharing of excess energy between the tunnelled electron and the bound electrons takes some time, resulting in a time delay on attosecond time scale between recollision and ionization. Our simulation upholds this picture of attosecond electron thermalization: on upper panel of Fig. 8, two bright spots are observed at a similar time delay on subfemtosecond time scale for CI trajectory.

The regular pattern in Fig.8(a),(c) exhibit that the ejection of electrons in the same-hemisphere and opposite-hemisphere emerge alternately with respect to the delayed time. For a time delay of odd half laser cycles, two electrons are emitted in the same direction, for

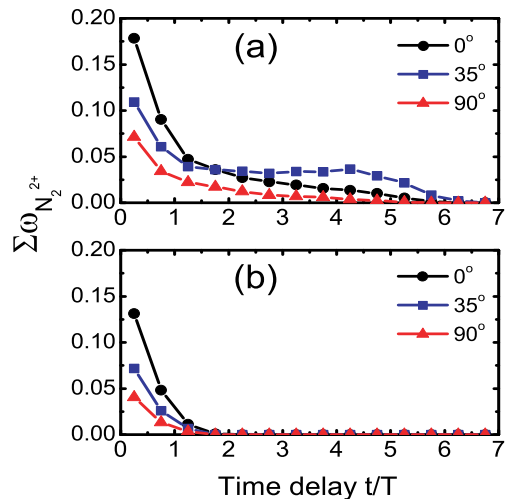


FIG. 9: (color online). DI yield versus the delayed time at laser intensity of 0.15PW/cm². The total optical cycles is (a)7, (b)3, respectively.

a time delay of even half laser cycles, two electrons are emitted back-to-back. Moreover, in the tunneling regime the pattern in Fig.8(a) shows two notably bright spot in the first and third quadrants when the delayed time is less than 0.5T, a phenomenon directly due to the CI trajectories. On the other hand, the irregular pattern emerges in Fig.8(b) for DI in the plateau regime as the signature of complicated multiple-collision trajectories. It implies that the trajectories of two electrons entangle with each other before DI ionization occurs and the electrons' motion might be chaotic [34].

Integrating over angle in Fig.8 gives total DI yield vs the delayed time as illustrated in Fig.9, where a laser field with seven and three optical cycles is used in (a) and (b), respectively. In each case, we also choose three alignment angles, i.e. 0°, 35° and 90° for comparison. As known to all, a DI event with delayed time less than 0.5T represents CI trajectory while others are all CEI trajectories. In Fig.9(a), both CI and CEI are suppressed for perpendicular molecules compared with parallel ones. However, for the case of 35°, CEI play a more important role than other two cases. As a result, the total number of CI and CEI events stays almost unchanged and forms the quasi-plateau between [0°,35°] in Fig.5(a). This plateau can be eliminated by using shorter laser pulses because the excessive CEI can be effectively suppressed as demonstrated in Fig.5(b).

V. CONCLUSIONS

In summary, we have developed a semiclassical quasi-static model with including classical rescattering and quantum tunneling effects and achieved insight into the dynamics of two highly-correlated valence electrons un-

der the combined influence of a two-center Coulomb potential and an intense laser field. Our model can be used to compared with experimental data of molecular DI quantitatively under the relevant experimental conditions, i.e., highly nonperturbative fields with femtosecond or shorter time resolution. We reproduce the experimental data of the plateau structure of the DI, uneven DI yield for parallel or perpendicular aligned molecules, and the accumulation of the emitted electrons in the first and third quadrants of parallel momentum plane. In addition, our model calculation reveals some novel features, such as a shallow dip in the plateau regime, enhancement of anisotropy when illuminated by shorter laser pulses and the regular patterns of correlated momentum with

respect to the time delay. We hope our theory will stimulate the experimental works in the direction.

VI. ACKNOWLEDGMENTS

This work is supported by NNSF of China No.10574019, CAEP Foundation 2006Z0202, and 973 research Project No. 2006CB806000. We thank J. H. Eberly for stimulating discussions. In particular, we are indebted to X. Liu for very useful discussions and suggestions.

-
- [1] M. Protopapas, C. H. Keitel, and P. L. Knight, Rep. Prog. Phys. **60**, 389 (1997).
- [2] *Atoms in Intense Laser Fields*, edited by M. Gavrilu (Academic, New York, 1992).
- [3] B. Walker, B. Sheehy, L. F. DiMauro *et al.*, Phys. Rev. Lett. **73**, 1227 (1994); Th. Weber *et al.*, Nature **405**, 658 (2000); X. Liu, H. Rottke, E. Eremina *et al.*, Phys. Rev. Lett. **93**, 263001 (2004), and references therein.
- [4] L. D. Landau and E. M. Lifshitz, *Quantum Mechanics* (Pergamon Press, New York, 1977).
- [5] D. N. Fittinghoff, P. R. Bolton, B. Chang and K. C. Kulander, Phys. Rev. Lett. **69**, 2642 (1992).
- [6] P. B. Corkum, Phys. Rev. Lett. **71**, 1994 (1993).
- [7] T. Brabec, M. Y. Ivanov, and P. B. Corkum, Phys. Rev. A **54**, R2551 (1996).
- [8] Th. Weber *et al.*, Phys. Rev. Lett. **84**, 443 (2000); R. Moshhammer *et al.*, Phys. Rev. Lett. **84**, 447 (2000); A. Becker and F. H. M. Faisal, Phys. Rev. Lett. **84**, 3546 (2000); M. Lein *et al.*, Phys. Rev. Lett. **85**, 4707 (2001).
- [9] C. Guo, M. Li, J. P. Nibarger, and G. N. Gibson Phys. Rev. A **58**, R4271 (1998).
- [10] C. Cornaggia and Ph. Hering, Phys. Rev. A **62**, 023403 (2000).
- [11] J. Muth-Böhm, A. Becker, and F. H. M. Faisal, Phys. Rev. Lett. **85**, 2280 (2000).
- [12] T. K. Kjeldsen and L. B. Madsen, J. Phys. B: At. Mol. Opt. Phys. **37**, 2033 (2004).
- [13] A. S. Alnaser, S. Voss, X. M. Tong *et al.*, Phys. Rev. Lett. **93**, 113003 (2004)
- [14] E. Eremina, X. Liu, H. Rottke *et al.*, Phys. Rev. Lett. **92**, 173001 (2004)
- [15] D. Zeidler, A. Staudte, A. B. Bardon, D. M. Villeneuve, R. Dörner, and P. B. Corkum, Phys. Rev. Lett. **95**, 203003 (2005).
- [16] J. S. Parker *et al.*, J. Phys. B **33**, L691 (2000).
- [17] A. I. Pegarkov, E. Charron and A. Suzor-Weiner, J. Phys. B **32**, L363(1999).
- [18] A. Becker and F. H. M. Faisal, J. Phys. B **38**, R1 (2005).
- [19] Jakub S. Prauzner-Bechcicki, Krzysztof Sacha, Bruno Eckhardt, and Jakub Zakrzewski, Phys. Rev. A **71**, 033407 (2005).
- [20] J. Liu, D. F. Ye, J. Chen, and X. Liu, Phys. Rev. Lett. **99**, 013003 (2007).
- [21] The atomic ADK theory has been extended to diatomic molecules; see, for example, X. M. Tong *et al.*, Phys. Rev. A **66**, 033402 (2002) and I. V. Litvinyuk *et al.*, Phys. Rev. Lett. **90**, 233003 (2003). An explicit analytic expression has also been derived in [22]. However, we found that the employment of atomic ADK formula instead of the complicated molecular ADK formula does not lead to significant discrepancy in calculating the ratios between double and single ionization. So, for simplicity, we adopt $\varpi(t_0) = \frac{4(2I_{p1})^2}{\varepsilon(t_0)} \exp(-\frac{2(2|I_{p1}|)^{3/2}}{3\varepsilon(t_0)})$ in our calculations.
- [22] Y. Li, J. Chen, S. P. Yang, and J. Liu, 'Correlated momentum distribution of double-ionized molecules', to appear in Phys. Rev. A (2007).
- [23] R. Abrines and LC. Percival, Proc. Phys. Soc. London **88**, 861 (1966); J. G. Leopold and I. C. Percival, J. Phys. B **12**, 709 (1979).
- [24] Li-Bin Fu, Jie Liu, Jing Chen, and Shi-Gang Chen Phys. Rev. A **63**, 043416 (2001); J. Chen, J. Liu, L. B. Fu, and W. M. Zheng Phys. Rev. A **63**, 011404 (2001); Li-Bin Fu, Jie Liu, and Shi-Gang Chen Phys. Rev. A **65**, 021406 (2002); J. Chen, J. Liu, and W. M. Zheng Phys. Rev. A **66**, 043410 (2002).
- [25] Jie Liu and Jing Chen, Chin. Phys. Lett. **23** 91 (2006).
- [26] L. Meng, C. O. Reinhold and R. E. Olson, Phys. Rev. A **40**, 3637 (1989).
- [27] S. L. Haan, L. Breen, A. Karim, and J. H. Eberly, Phys. Rev. Lett. **97**, 103008 (2006), and references therein.
- [28] B. Walker *et al.*, Phys. Rev. Lett. **73**, 1227 (1994); B. Walker *et al.*, Phys. Rev. Lett. **77**, 5031 (1996).
- [29] G. G. Paulus, W. Becker, W. Nicklich and H. Walther, J. Phys. B **27**, L703 (1994).
- [30] J. S. Parker, B. J. S. Doherty, K. J. Meharg, and K. T. Taylor, J. Phys. B **36**, L393 (2003).
- [31] B. Feuerstein, R. Moshhammer, D. Fischer *et al.*, Phys. Rev. Lett. **87**, 043003 (2001).
- [32] M. Weckenbrock, D. Zeidler, A. Staudte *et al.*, Phys. Rev. Lett. **92**, 213002 (2004).
- [33] X. Liu, C. Figueira de Morisson Faria, W. Becker and P. B. Corkum, J. Phys. B **39**, L305 (2006).
- [34] B. Hu, J. Liu and S.G. Chen, Phys. Lett. A **236**, 533 (1997)